VOL. IX MARCH, 1922 No. 3

THE BROWN BOVERI REVIEW

EDITED BY BROWN, BOVERI & CO., BADEN (SWITZERLAND)

VALLE BREMBANA RAILWAY. FREIGHT TRAIN NEAR LISSO.

CONTENTS:

BROWN BOVERI

A.C. AND D.C. SWITCHGEAR

FOR ALL OUTPUTS AND PRESSURES

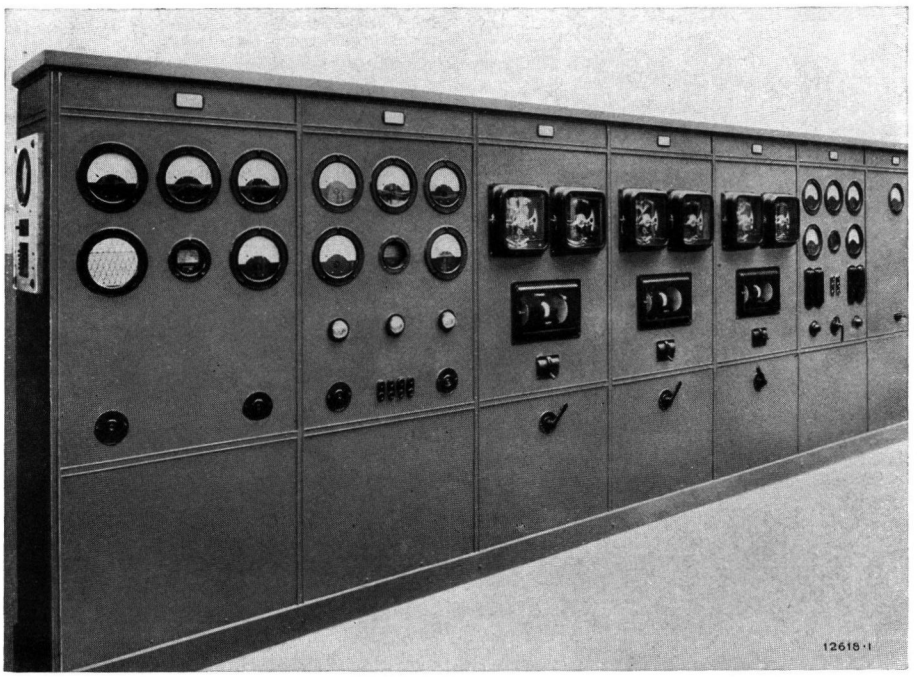

LAUSANNE MUNICIPAL ELECTRIC SUPPLY. HYDRO-ELECTRIC POWER STATION AT BOIS-NOIR, NEAR ST. MAURICE.
Panels with automatic current and voltage regulators for the alternators.

SWITCH-BOARDS - SWITCH-DESKS
SWITCH-COLUMNS - SWITCH-BOXES

THE BROWN BOVERI REVIEW

THE HOUSE JOURNAL OF BROWN, BOVERI & CO., BADEN (SWITZERLAND)

VOL. IX MARCH, 1922 No. 3

The Brown Boveri Review is issued monthly. Single numbers: 1.20 francs (1 shilling). Yearly subscription: 12 francs (10 shillings).

SINGLE-PHASE LOCOMOTIVES FOR THE VALLE BREMBANA RAILWAY.

Decimal index 621. 331. 34 (45).

THE Valle Brembana Railway runs from Bergamo in Lombardy to San Giovanni Bianco, which lies to the north, and passes through San Pellegrino, a flourishing summer resort. Shortly after leaving Bergamo the line enters the lovely Brembo valley, which it follows all the rest of the way.

The railway deals with both passenger and freight traffic, and is about 30 km long. The line is single track, 1445 mm gauge, laid independently of the roads, and has many short tunnels, as well as bridges over the Brembo and its tributaries. The steepest gradient is 2·4 % and the sharpest curves 150 m radius in the open and 120 m at points. The weight of the rails is 27·6 kg per m, while the permissible static axle load is 10·7 metric tons.

On account of the facility with which hydro-electric power can be obtained from the Brembo, electric traction was decided upon from the start. After exhaustive studies single-phase current was adopted.

A hydro-electric power station situated on the Brembo about one km above San Giovanni Bianco feeds the line. The power station contains three units each composed of a water turbine and a single-phase alternator for 500 kVA continuous output, 6000 V, 25 cycles. The overhead contact wire of grooved copper and with a cross-section of 50 sq. mm is attached to the overhead structure by means of a catenary suspension. It is normally 6·0 m above the track, this distance being increased to 6·5 m in stations and at level crossings, and reduced to 4·5 m in tunnels. The poles also carry a copper feeder wire of the same cross section as the contact wire.

The line was opened in 1907, and the traffic increased to such an extent that the original rolling stock had to be supplemented by two further locomotives of a more powerful type. The contract for these was placed with the Tecnomasio Italiano Brown Boveri, Milan. Delivery was greatly delayed through the war, and the locomotives were put into service only recently.

Although these locomotives have been built to plans prepared at the beginning of the war, a short description will not be out of place as it deals with a type of locomotive designed for conditions (contact-wire voltage and frequency) often met with in many of the earlier single-phase lines.

GENERAL.

The locomotives were specified for a tractive effort of 5100 kg at the tread of the wheels on a one hour rating, the speed being 20 km per hour. They were to be capable of hauling from Bergamo to San Giovanni Bianco, or vice versa, freight trains weighing 150 metric tons in about 1½ hours not including intermediate stops, or passenger trains weighing 88 t in 1 hour 10 min including seven intermediate stops of one minute each.

The locomotives had to be designed for a maximum speed of 40 km per hour.

On account of these requirements and the permissible axle load, 0-4-4-0 locomotives with a total motor capacity of 400 H. P. on a one hour rating were decided upon. The principal particulars of these are as follows: —

Length over buffers	12 400 mm.
Length of body	5560 mm.
Width of body	2900 mm.
Height of roof above rails	3650 mm.
Total wheelbase	9400 mm.
Bogie wheelbase	2600 mm.
Distance between bogie centres	5900 mm.
Diameter of coupled wheels	1100 mm.
Maximum axle load	10·7 metric tons.
Total weight of locomotive	42·8 „ „
Weight of mechanical part	25·8 „ „
Weight of electrical equipment	17 „ „

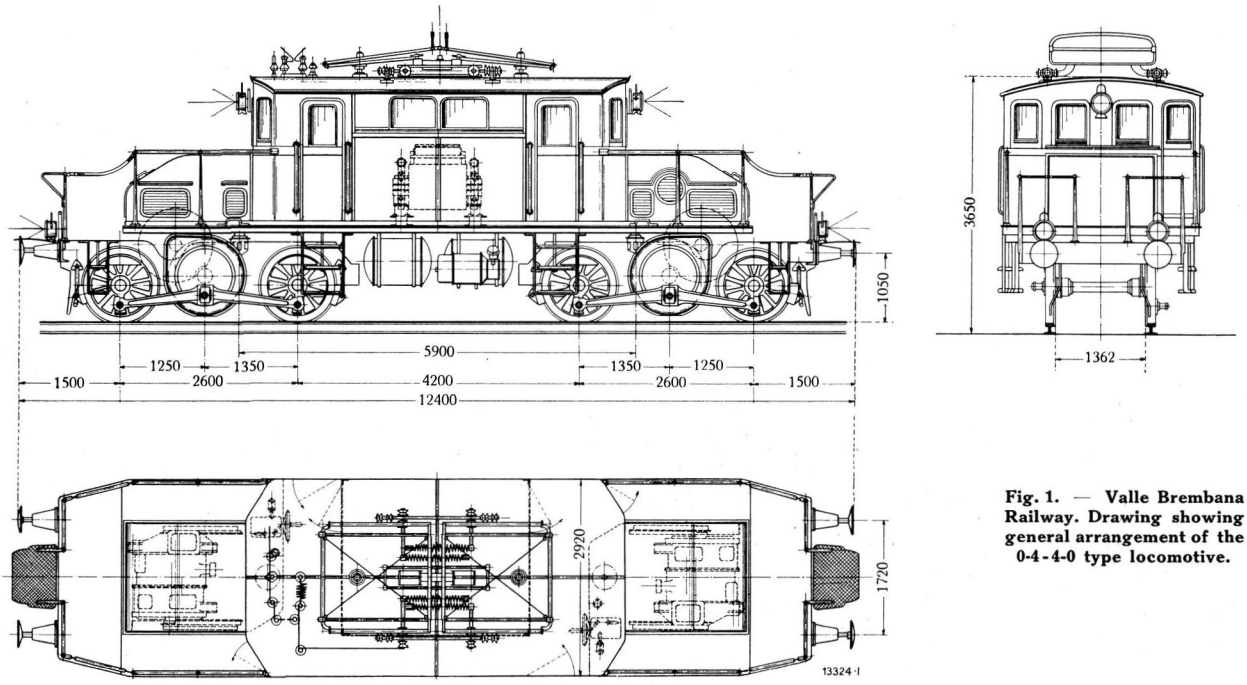

Fig. 1. — Valle Brembana Railway. Drawing showing general arrangement of the 0-4-4-0 type locomotive.

MECHANICAL PART.

The mechanical part (Figs. 1 and 2) comprises the two bogies, the underframe and the body with two sloping ends. Each bogie consists of a frame mounted on two axles. Between and slightly higher than the axles is a jackshaft which transmits the power from the motor, this latter being also mounted on the bogie frame. The twin gear wheels on the jackshaft serve at the same time as crank discs, the crank pins of which engage in a slide on the coupling rods. The gear ratio is 1 to 5·69, single helical gears being used. The gear teeth at one end of the motor are right-hand and at the other left-hand in order to obviate axial pressure on the shaft. Neither the pinions nor the spur wheels are provided with elastic spring gear. The rims of the spur wheels are removable.

Each bogie is fitted with the standard Italian State Rys. drawgear and buffers. The body has two sloping ends which protect the traction motors. Each end is provided with running boards and a communication gangway. The central part of the body is occupied by the H. T. equipment (the transformer and the principal apparatus). At each end there is a driver's cab (Fig. 3), from which a door gives access to the running boards and the gangway. Communication between the two cabs is possible by means of an open passage at one side of the H. T. compartment. To allow of access to the latter, doors and openings are provided, which are locked in such a way that they can only be opened when the current collector is lowered. A grounding switch, connected to the lock, grounds the H. T. equipment as soon as this compartment is opened. One side of the latter, as well as part of the corresponding side of the locomotive body, are removable to allow of taking out the transformer with its tapping switch.

The locomotive body rests on an underframe uniting the bogies which also transmits the tractive effort.

Braking is effected by eight brake shoes. The rigging can be operated from each end either by a hand screw or by the Westinghouse quick-acting brake equipment. A speed-indicator is fitted to each driver's cab, and air sanding is provided for each bogie.

The mechanical part is similar to that of the locomotives of the Burgdorf-Thun Ry., described on a previous occasion (Revue BBC, No. 3/4, BBC Mitteilungen, No. 4, 1919).

The mechanical part of these two locomotives was built by E. Breda, Locomotive Works, Milan, to plans furnished by the Tecnomasio Italiano Brown Boveri.

ELECTRICAL EQUIPMENT.

As neither multiple-unit electric control nor electric braking were required, the electrical equipment could be kept very simple. All the main apparatus, including the pantograph collector, are oper-

ated by compressed air. Special mention may be made of the following apparatus in the H.T. circuit: —

The main oil-switch has four breaking points with auxiliary contact and switching-in resistances. It is provided with an overload release with free return clutch, as well as directly built-on pneumatic control gear. Switching in and out can be done by hand if necessary.

The transformer (Fig. 4). On account of the relatively low voltage an air-cooled transformer with forced draught was adopted. The H. T. and L. T. windings are quite separate from one another. The main winding on the L. T. side has 10 tappings giving tensions from 80 to 336 V for the traction motors. There are also two auxiliary L. T. windings, one of which feeds the auxiliary service circuit at 105 V, while to the other are connected the voltmeters and the pressure coil of the wattmeter. The above tensions (80 to 336 and 105 V) correspond to full load of the motors and apparatus. The one hour rating of the transformer is 410 kVA and the continuous output 360 kVA, both for a transforming ratio of about 6000/270 V at 25 cycles. For auxiliary service (air compressor, fan for the forced draught, train lighting and heating of the driver's cab) the transformer can give an additional 20 kVA.

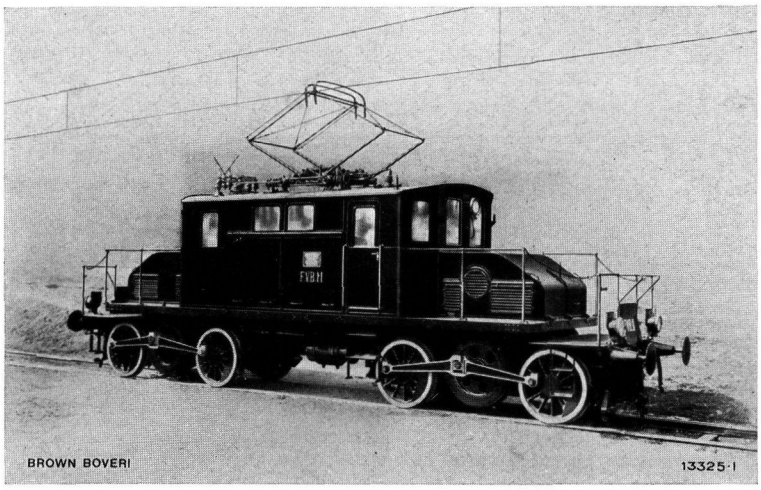

Fig. 2. — Valle Brembana Railway. 0-4-4-0 locomotive.

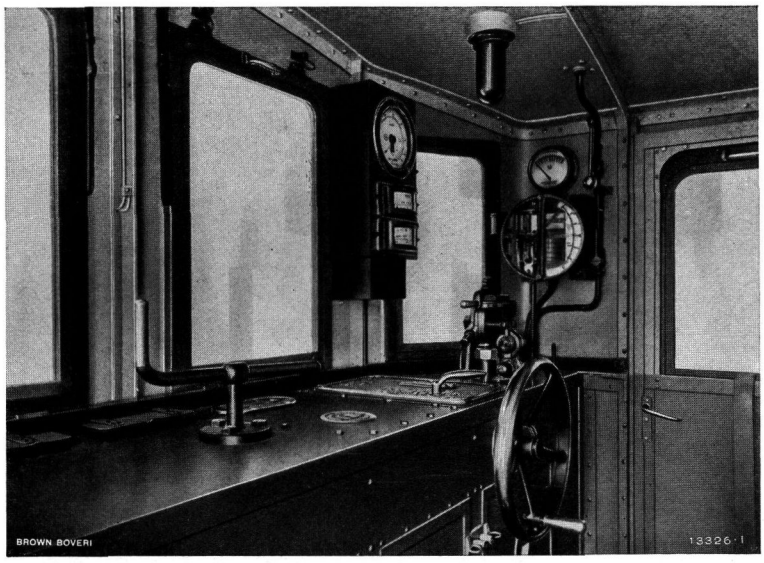

Fig. 3. — Valle Brembana Railway. View of driver's cab, 0-4-4-0 locomotive.

Among the apparatus in the circuit of the traction motors are: —

The tapping switch which has a built-on sparking-switch and a step resistance. This apparatus is of a type which has proved very satisfactory on many other Brown Boveri single-phase locomotives (Revue BBC or BBC Mitteilungen, Nos. 6 and 9, 1921), and serves to connect the motors with the successive L. T. tappings of the transformer for adjusting the terminal voltage of the motors as required for starting or for speed regulation. As already mentioned, the transformer has 10 L. T. tappings, and the tapping switch, which is mounted on the transformer, has the same number of positions. This number of steps, although small compared with many other designs, is sufficient for the relatively low power and running speeds required in the present case.

The normal tension at the motor terminals is reached on the eighth step and the two last steps serve to compensate the voltage-drop in the contact wire up to a maximum of 20 %. The tapping switch is operated by a dummy controller in each driver's cab by means of chain transmission and an intermediate shaft supported in ball bearings. One turn of the handwheel of the dummy controller corresponds to one step on the tapping switch.

The L. T. oil-switch. This serves to protect the two motors from overloads, and is consequently fitted with an overload release. It has further a free

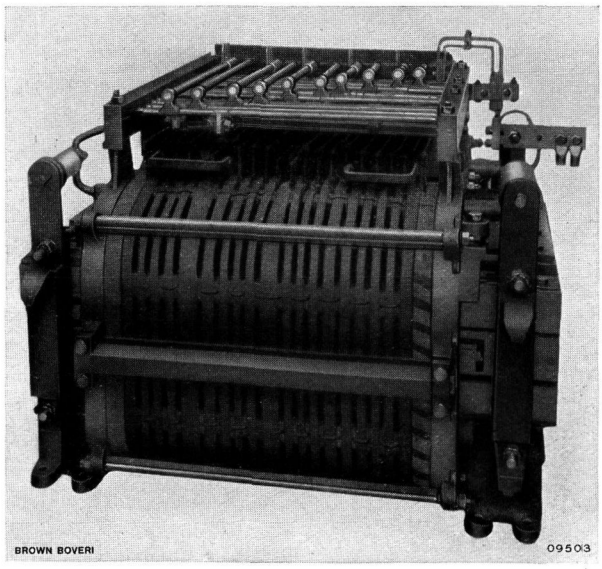

Fig. 4. — Valle Brembana Railway. Air-cooled transformer for the 0-4-4-0 locomotives.

return clutch and can be operated pneumatically or by hand. In case of emergency the switch can be opened from the driver's cabs by merely pressing a push-button which closes the circuit of a tripping voltage coil. Thus the L. T. switch alone allows the traction motors to be switched off quickly in case of need, without extinguishing the lights on the locomotive or in the train.

Reversing switches. These also are pneumatically operated and have only two positions, viz., forward and reverse. The operating valves in the driver's cabs are interlocked with the dummy controller in such a way that:

(a) The reversing switch can only be thrown over when the dummy controller is in the zero position, and

(b) This latter can only be operated when the reversing switch is in either the forward or the reverse position.

The traction motors (Fig. 5), are 12-pole compensated single-phase series motors with resistances between armature windings and commutator. Each motor has the following outputs measured at the shaft —

115 H. P. continuously and 200 H. P. on a one hour rating, both at 550 r. p. m. (corresponding to 20 km per hour), with a maximum temperature rise of 75 ^{0} C for all parts, measured thermometrically or by increase of resistance.

The two motors are permanently connected in parallel, but each of them can be disconnected singly from the circuit by separate knife switches if necessary.

AUXILIARY EQUIPMENT.

The auxiliary motors, train lighting and locomotive heating are fed from a separate transformer tapping at 105 V. The air compressor is of the standard Brown Boveri E C 3 type driven by a Deri motor. The fan for cooling the transformer is coupled to an ordinary single-phase series motor. As these locomotives are intended chiefly for freight traffic and are only used on passenger trains at busy periods in the summer, the transformer supplies current for lighting the train only and not for heating. Carbon filament lamps are used on account of the steadier illumination they give with the low frequency of 25 cycles as they have a larger heat capacity than metallic filament lamps. For heating in the locomotive cabs hot foot-plates are provided.

The electrical equipment of the above two locomotives was built in the Milan workshops of the Tecnomasio Italiano Brown Boveri. The locomotives were put into regular service in the beginning of 1921.

Brodbeck. (D. M.)

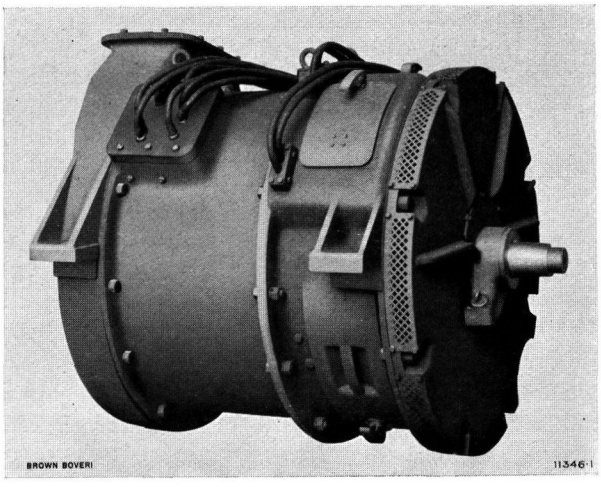

Fig. 5. — Valle Brembana Railway. Completed 12-pole traction motor for the 0-4-4-0 locomotives.

LOSSES IN THE NOZZLES AND BLADING OF STEAM TURBINES.

Decimal index: 621. 165. 13.

III. RESULTS OF EXPERIMENTS.[1]

(A) NOZZLES.

NOZZLES of circular and rectangular cross-section having mouths normal or oblique to the nozzle axis were experimented with. Firstly, the discharge coefficient χ was determined. (A nozzle having a cross-section of f_m sq. m at the throat has a discharge G kg/sec given by: $G = \chi f_m \sqrt{\frac{p_1}{v_1}}$ when the back pressure is lower than the critical pressure). The discharge of the nozzle was then known when delivering into a vacuum when measuring experimentally the exact reaction of the steam jet. These measurements were made with constant initial pressure and temperature, the back pressure being variable. The reactive force was expressed as a function of the back pressure, and it was then possible to deduce immediately the nozzle characteristic.

The average deviation from the nozzle axis of the steam jet on leaving the nozzle was also determined by means of two reaction measurements for nozzles having outlets oblique to their axis.

For measuring the static pressure the walls of the nozzles were provided with carefully rounded-off holes. With certain nozzles having a circular cross-section the rate of flow in the axis was determined with the aid of a Pitot tube.

The coefficient of friction was measured in a number of tests for rates of flow up to 1200 m per sec. Previously this determination had only been made for rates of flow below the velocity of sound, therefore it was of interest to have some results for velocities above this latter limit.

Another series of tests was undertaken to determine the extent of supersaturation at the mouth of the nozzles.

The principal results of these tests are given below.

It is evident, that in an article dealing with such a comprehensive subject, it is impossible to go into every detail. These experiments were undertaken to obtain data of technical importance. Several questions of purely academical interest are only briefly dealt with.

The following symbols are used:—

c_1 = actual rate of flow.
c_0 = rate of flow for an adiabatic expansion.
f_2 = area of the mouth.
f_m = area of the throat.
f_x = an area.
G = discharge per unit of time.
g = acceleration due to gravity (m/sec^2).
n = a constant.
p_2 = pressure on leaving the nozzle.
p_c = back pressure.
R = reactive force.
r = radius of the nozzle.
t_1 = temperature before the nozzle.
v_1 = specific volume before the nozzle.
w = rate of flow in the nozzle at a distance ρ from the nozzle axis.
w_0 = rate of flow in the nozzle axis.
a = ratio of the areas $\frac{f_2}{f_m}$.
β_0 & β_1 = constants.
γ_1 = specific weight of the steam near the walls of the nozzle.
γ_0 = specific weight of the steam in the nozzle axis.
φ = nozzle coefficient $\varphi = \frac{c_1}{c_0}$.
α_1 = convergence of nozzle.
Δi = heat drop.
k = adiabatic expansion exponent $= \frac{c_p}{c_v}$.
λ = $\frac{\gamma_0}{\gamma_1}$.
χ = discharge coefficient.
$\frac{wd}{\nu}$ = Reynolds coefficient.
ρ_{abs} = coefficient of viscosity in absolute units.

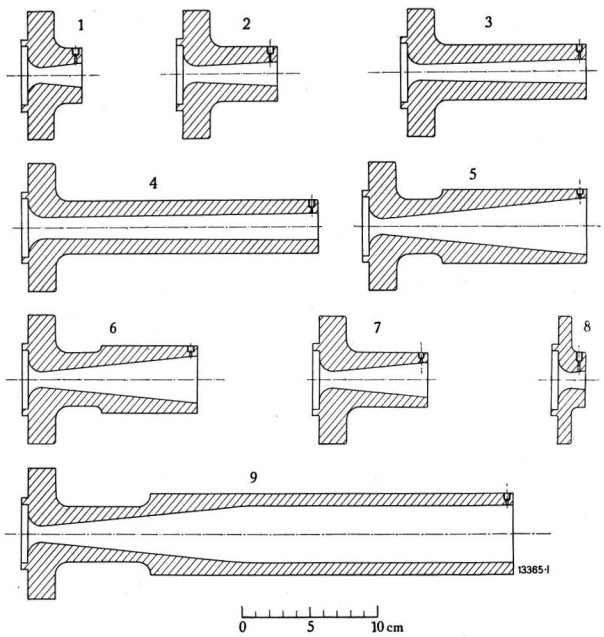

Fig. 21. — Nozzles Nos. 1—9 used for the tests.

[1] For a description of the apparatus used see Revue BBC or BBC Mitteilungen, No. 10, 1921.

I. EXPANDING NOZZLES HAVING A CIRCULAR CROSS SECTION.

The nozzles experimented with are shown in Fig. 21. It will be noticed that the length of the nozzle as well as the divergence is variable, it being then possible to determine the influence of the divergence and of the friction on the walls.

(a) Value of the discharge coefficient.

Each nozzle was calibrated for various initial pressures and temperatures. Table I gives the measured values of the discharge coefficient

$$\chi = \frac{G}{f_m \sqrt{\frac{p_1}{v_1}}}$$

from which the average value $\chi = 2{\cdot}056$ can be deduced.

TABLE I.

Nozzle No.	χ	Nozzle No.	χ
1	2·062	5	2·070
2	2·065	6	2·050
3	2·051	7	2·052
4	2·054	8	2·050

The exact area of the throat f_m was very difficult to measure with the means at disposal and the discrepancies in the table are therefore due to small errors in this measurement. In order to eliminate this error, the value of χ obtained for a given nozzle will always be used in calculations referring to this nozzle.

Bendemann[1], by means of very carefully carried out experiments, found an average value of $\chi = 2{\cdot}031$. On comparing the figures obtained by the above mentioned tests with this value, it will be noticed that the results differ by 1 %; Bendemann, however, used old steam tables for his researches. On recalculating his data with the latest steam tables[2] an average value for 20 measurements of $\chi = 2{\cdot}054$ is found. This value agrees very closely with the average value given above.

For expanding nozzles having a circular cross-section χ may be taken as being equal to 2·055.

If superheated steam obeys the laws of a perfect gas[1] then

$$\chi = \sqrt{2\,g\,\frac{k}{k+1}\left(\frac{2}{k+1}\right)^{\frac{2}{k-1}}}$$

If the adiabatic expansion exponent k is taken equal to 1·3 the discharge coefficient becomes

$$\chi = 2{\cdot}090$$

This theoretical value is 1·7 % greater than the average experimental figure. The difference is not exclusively due to the friction of steam on the nozzle walls, as will be shown in a later chapter.

Superheated steam does not, in reality, obey exactly the laws governing a perfect gas; this may also influence the value of the discharge coefficient. To find out the discrepancy an entropy diagram was used as follows (Fig. 22):—

From the initial point (p_1, t_1) draw the straight line corresponding to an adiabatic expansion. For any pressure p_x

$$G\,v_x = f_x\,w_x$$

$$G = f_x \frac{w_x}{v_x}$$

w_x is determined by the adiabatic heat drop Δi_x as $w_x = 91{\cdot}5\sqrt{\Delta i_x}$

For a certain value of $p_x = p_k$ the ratio $\frac{w_x}{v_x}$ is a maximum, the section $f_x = f_m$ is a minimum and

$$G = \chi\, f_m \sqrt{\frac{p_1}{v_1}}$$

which gives

$$\chi = \sqrt{\frac{v_1}{p_1}}\left(\frac{w}{v}\right)_{max} \qquad (11)$$

χ was calculated this way for a considerable number of points. The values obtained varied from 2·080 to 2·110. The position on the entropy diagram does not seem to affect the values, and the discrepancies are probably due to small errors in reading. The theoretical value $\chi = 2{\cdot}090$ is therefore retained.

For saturated steam, the same value for the discharge coefficient was found, namely $\chi = 2{\cdot}055$ in agreement with Bendemann. This is due to supersaturation of saturated steam in the first part of the nozzle. This question will be further examined later on.

[1] Forschungsarbeiten, published by the Verein deutscher Ingenieure, No. 37.

[2] Stodola: "Dampfturbinen," fifth edition. Prof. Stodola kindly put these tables at our disposal before the publication of this work.

[1] This calculation is given for instance in Ewing: "Thermodynamics for Engineers", p. 196.

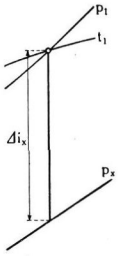

Fig. 22.

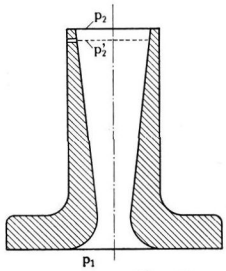

Fig. 23.

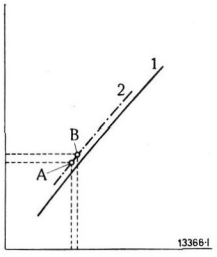

Fig. 24.

Fig. 22. — Expansion represented on an entropy diagram.

Fig. 23. — Arrangement for measuring the pressure near the nozzle mouth.

Fig. 24. — Determination of the pressure at the nozzle mouth, the pressure near the nozzle mouth having been measured.

Ordinates: f_2/f_m = surface ratio. Abscissæ: p_1/p_2 = pressure ratio.

(b) The pressure ratio $\frac{p_1}{p_2}$.

For measuring the pressure near the mouth, a hole, well rounded-off, was bored as near as possible to it through the nozzle wall (Fig. 23). It was then possible to measure the pressure p'_2 at a section f'_2 near the mouth; p_2 and f_2 are the respective values at the mouth. As these two pressures only differ by a small amount, p_2 can be determined as follows:—

The theoretical curve (1, Fig. 24) giving $\frac{f_2}{f_m}$ as a function of $\frac{p_1}{p_2}$ being known as well as (A) — the latter point is determined by the values of p'_2 and f'_2 — draw through (A) a curve (2) similar to (1). This curve gives immediately (B), i. e., $\frac{p_1}{p_2}$ and the real value of p_2 at the mouth.

The pressure ratios measured this way for saturated steam are given in Table II.

TABLE II.

Nozzle No.	f_2/f_m	p_1/p_2	p_1/p_2 (adiabatic)
1	2·25	8·16	9·25
2	2·25	7·78	9·25
3	2·28	7·73	9·40
4	1·572	4·20	5·25
5	12·03	80·07	85·0
6	8·40	51·2	54·2
7	4·71	24·3	25·8
8	1·345	4·45	3·90

With nozzles Nos. 1, 2 and 3 it is seen that the pressure ratio varies when the length of the nozzle, i. e., the resistance, increases, the ratio of the cross-sections remaining unaltered.

The initial temperature t_1 also has an effect on the pressure ratio; for nozzle No. 5 (Fig. 21) with a surface ratio of 12·03 the following values were obtained:—

t_1	p_1/p_2
saturation	80·07
250° C	83·56
300° C	88·46

These results are explained as follows:—

For an adiabatic expansion, the following relation between $\frac{p_1}{p_2}$ and $\frac{f_2}{f_m}$ may be written:—

$$\frac{f_2}{f_m} = \sqrt{\frac{k-1}{k+1}} \left(\frac{2}{k+1}\right)^{\frac{1}{k-1}} \sqrt{\frac{(p_1/p_2)^{\frac{k+1}{k}}}{(p_1/p_2)^{\frac{k-1}{k}} - 1}} \qquad (12)$$

Taking $k = 1{\cdot}30$ for superheated steam and $k = 1{\cdot}135$ for saturated steam, the curves designated by $\varphi = 1$ were obtained (Fig. 25).

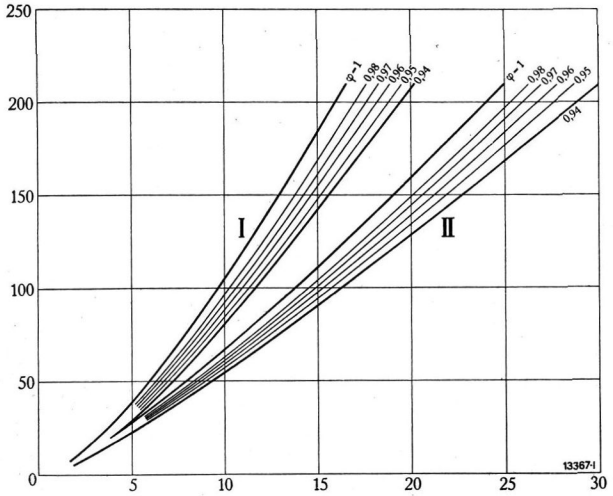

Fig. 25. — Pressure ratios as a function of the surface ratio for different values of the nozzle coefficient.

I. For superheated steam, II. For saturated steam.

Ordinates: f_1/f_m = surface ratio. Abscissæ: p_1/p_2 = pressure ratio.

If the expansion is not adiabatic, the leaving velocity will be smaller on account of losses. In order to pass the same weight of steam through the nozzle, the specific volume, i. e., the pressure, must be greater. On account of the losses, the pressure ratio is also smaller. Table II shows that the pressure ratio for adiabatic expansion is generally greater than the ratio measured. Nozzle No. 8 is an exception, in this case, however, the supersaturation undoubtedly affects the results.

It has been possible to show — by means of measurements with a Pitot tube — that the rate of flow near the nozzle axis is practically equal to the velocity produced by a corresponding adiabatic expansion. Consequently, losses are principally due to friction near the nozzle walls, where the rate of flow drops rapidly. The velocity distribution in a cross section is given in Fig. 2. (Revue BBC, No. 2/3 or BBC Mitteilungen, No. 3/4, 1921.)

Stodola[1] uses the following formulæ for nozzles having circular cross-sections:—

$$w = w_0 \left[1 + \left(\frac{\rho}{r} \right)^n \right] \qquad (13)$$

$$\gamma = \gamma_1 + (\gamma_0 - \gamma_1) \frac{w}{w_0} = \gamma_0 \left[\lambda + (1 - \lambda) \frac{w}{w_0} \right] \qquad (14)$$

where

$$\lambda = \frac{\gamma_1}{\gamma_0}$$

Then

$$G = \int_0^r 2 \pi \rho \cdot d\rho \cdot \gamma w = \beta_0 f_2 w_0 \gamma_0$$

where

$$\beta_0 = \frac{n^2}{(n+1)(n+2)} \left(1 + \frac{\lambda}{n} \right)$$

The reactive force

$$R = \int_0^r 2 \pi \rho \frac{\gamma}{g} w^2 \cdot d\rho = \beta_1 f_2 w_0^2 \frac{\gamma_0}{g}$$

where

$$\beta_1 = \frac{n^3}{(n+1)(n+2)(3n+2)} (2\lambda + 3n)$$

Let φ be the nozzle coefficient as determined by reaction measurements, then

$$\varphi = \frac{\beta_1}{\beta_0} = \frac{n(2\lambda + 3n)}{(3n+2)(\lambda + n)} \qquad (15)$$

This equation gives n as a function of φ.

Let f_{2A} be the area of the mouth for an adiabatic flow $f_2 = \frac{f_{2A}}{\beta_0}$

The diagrams (Figs. 26 and 27) give n as a function of φ and β_0 with λ as parameter. If λ is known, β_0 can be deduced as a function of φ (Fig. 28) and

[1] Stodola: "Neue Versuche über die Unterkühlung beim Ausflusse gesättigten Dampfes", Schweizer. Bauzeitung, 1914, p. 168.

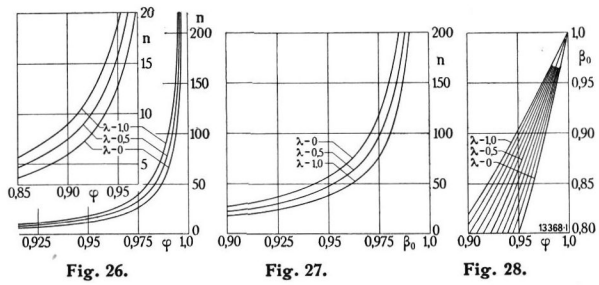

Fig. 26. Fig. 27. Fig. 28.

Fig. 26. — Expansion exponent n as a function of the nozzle coefficient φ in two different scales.

Fig. 27. — Exponent n as a function of the constant β_0.

Fig. 28. — β_0 as a function of the nozzle coefficient φ.

the ratio of the areas corresponding to given nozzle losses can be determined. λ, however, is not constant but varies according to the pressure ratio. Fig. 29 shows the variations of λ for varying pressure ratios, the initial pressure being 15 at. abs. The curves given in Fig. 25 are calculated in this way.

All these deductions are naturally only valid for expansions where the steam is throughout either superheated or saturated (without supersaturation). For high pressure ratios this is usually not the case, the expansion taking place partly in the superheated partly in the saturated region; the pressure ratio is altered and, in this case, may be calculated with the help of an entropy diagram. As the high pressure ratios are no longer prevalent in modern turbines, it is not necessary to go into further details. On comparing Table II with Fig. 25, it will be noticed that for nozzles having the same divergence ($\operatorname{tg} \alpha_1 = 0{\cdot}1$), the coefficient φ seems nearly constant and equal to 0·98. The effect of supersaturation was not taken into account — doubtlessly it would influence the results. The determination of the nozzle coefficient φ by means of the pressure ratio is therefore not reliable.

(c) The nozzle characteristic.

This is a curve giving φ as a function of the pressure ratio or of the leaving velocity, the efficiency of a given nozzle varying with the pressure ratio. The *normal point* is the point on the φ curve for which the pressure at the mouth is equal to the back pressure. Two distinct zones exist on a diagram giving φ: —

(1) To the left of the normal point; the pressure ratio $\frac{p_1}{p_c}$ is smaller than the normal pressure ratio, i. e., there is *under-expansion;*

(2) To the right of the normal point; the pressure ratio is greater than the normal pressure ratio, i. e., there is *over-expansion.*

In the first instance, as is well known, there is a sudden compression accompanied by a considerable loss of energy before the mouth, consequently φ is very low and this zone has little technical interest.

In the second case very efficient expansion takes place after the jet has left the nozzle mouth, consequently the value of φ is high. This zone is much more interesting, especially as these conditions are encountered in practice, as for instance in turbines with nozzle control at partial loads.

Since Christlein's researches, over-expansion has been employed even at full load, as it is then possible to increase the efficiency and diminish the number of stages. Thorough research, in his matter will be of practical use.

Once the normal point is known the nozzle characteristic of a given nozzle is determined in the over-expansion zone. Let φ' be the value of φ at the normal point, the corresponding value of the reactive force is R′ and the heat drop $\Delta i'$. If the pressure drop is greater than normal, the heat drop increases as well as the reactive force. φ and R[1] have, in this case, the following values: —

$$\varphi = \frac{c_1}{c_0} = \frac{g\,R}{G \cdot 91{\cdot}5\,\sqrt{\Delta i}} \qquad (16)$$

$$R = R' + f_2\,(p_2 - p_c)$$

combining these two relations

$$\varphi = \frac{g}{G\ 91{\cdot}5\ \sqrt{\Delta i}}\left[R' + f_2\,(p_2 - p_c)\right] \qquad (17)$$

but

$$R' = \frac{G}{g}\,c' = \frac{G}{g}\,\varphi'\ 91{\cdot}5\ \sqrt{\Delta i'}$$

therefore

$$\varphi = \varphi'\sqrt{\frac{\Delta i'}{\Delta i}} + \frac{g\ f_2\ (p_2 - p_c)}{G\ 91{\cdot}5\ f\ \sqrt{\Delta i}} \qquad (18)$$

Let

$$f_2 = \alpha\ f_m$$

and

$$G = \chi\ f_m \sqrt{\frac{p_1}{v_1}}$$

which gives

$$\varphi = \frac{1}{\sqrt{\Delta i}}\left[\varphi'\sqrt{\Delta i'} + \frac{g\ \alpha\ (p_2 - p_c)}{\chi\ 91{\cdot}5\ \sqrt{p_1/v_1}}\right] \qquad (19)$$

[1] This formula was given in Revue BBC No. 2/3 or BBC Mitteilungen No. 3/4, 1921.

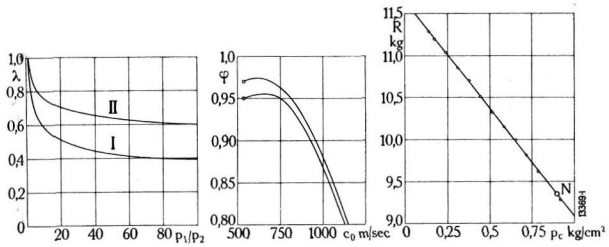

Fig. 29. **Fig. 30.** **Fig. 31.**

Fig. 29. — λ as a function of the pressure ratio.

I. For superheated or completely supersaturated steam.
II. For saturated steam.

Fig. 30. — Theoretical values of the nozzle coefficient φ as a function of the adiabatic rate of flow c_0.

Fig. 31. — Measured reactive force as a function of the back pressure.

For a given nozzle $\varphi'\sqrt{\Delta i'}$ and $\frac{g\,\alpha}{91{\cdot}5}\ \chi\ \sqrt{\frac{p_1}{v_1}}$ are constants which, for simplicity's sake, will be written as a and b respectively, therefore:

$$\varphi = \frac{a + b\ (p_2 - p_c)}{\sqrt{\Delta i}} \qquad (20)$$

Fig. 30 shows the values of φ as given by formula (20) for a converging nozzle; the initial state of the steam being 15 at. at 300° C. The pressure at the throat is then equal 8·8 at. abs. It will be seen that, to the right of the normal point, φ first increases and then decreases after having attained a maximum value. For $\varphi' = 0{\cdot}95$ this increase is greater than with $\varphi' = 0{\cdot}97$.

When the expansion continues outside the nozzle mouth, the area of the jet increases and radial velocity-components exist. The measurements of the reactive force, however, give the sum of the axial velocity-components only, the radial components being of no account. If the dispersion of the jet on leaving the nozzle is not too great, the radial components are small, and, at the same time, there is practically no friction of the jet on the walls. In this case the efficiency is high. The greater the friction in the nozzle, the greater the increase of φ after the normal point with over-expansion. If there were no nozzle losses, φ would be equal to unity at the normal point and decrease thereafter. Moreover, this explains Christlein's results. Also, the higher the adabiatic heat drop, the smaller the increase of φ to the right of the normal point, as, in formula (20) the numerator increases less rapidly than the denominator.

The results obtained by Brown Boveri fully confirm this variation of φ. For instance, Fig. 31 shows the reactive force as a function of the back pressure,

as measured with nozzle No. 3. The initial steam pressure was 6·92 at. abs. at 167 ° C; the discharge 0·1145 kg/sec. The points obtained lie on a straight line having an angular coefficient equal to:

$$\frac{\text{variation of the reactive force}}{\text{variation of the pressure}} = \frac{\text{kg}}{\text{kg/sq. m}}$$

i. e., an area equal to f_2, ($f_2 = 0{\cdot}000258$ sq. m). The results are in agreement with formula (10)[1]. N indicates the normal point.

The reactive force — as already been stated — can be measured very accurately with the apparatus used.

The reactive force as a function of the back pressure is therefore known. In order to determine the nozzle characteristic the heat drop corresponding to the various reactive forces has to be known. This was determined with the aid of Dr. Stodola's new entropy diagram in such a way as to render interpolation of the constant pressure curves unnecessary. The reactive forces corresponding to these back pressures could then be easily read on the straight lines in Fig. 31.

With nozzle No. 1 four different tests were made with saturated steam at various initial pressures. Fig. 32 gives the nozzle characteristic as a function of the pressure for this nozzle — the large scale was chosen for greater clearness. The discrepancies between the various characteristics attain only $^1/_4$ % and are probably due to errors in reading or irregularities in the entropy diagram. Therefore, the curves practically coincide, with saturated steam, and the nozzle characteristic appears to be independant of the initial state of the steam. It does not seem possible to establish, with the apparatus used, the influence of the initial pressure — if such an influence exists.

The characteristics for the nozzles Nos. 2 and 3 were determined in a similar way. Fig. 33 gives the characteristic for the three nozzles. The characteristics for nozzles Nos. 1 and 2 differ only slightly; with nozzle No. 3 the difference is more marked and is probably due to higher friction losses on account of its greater length. Attention may be drawn to the increase of φ to the right of the normal point with the three nozzles.

The influence of friction is still more apparent in the characteristic of nozzle No. 4. As might be expected on account of the considerable length of this

[1] See preceding footnote.

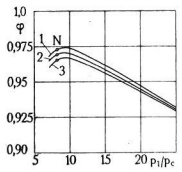

Fig. 32.

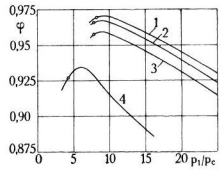

Fig. 33.

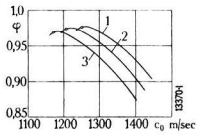

Fig. 34.

Fig. 32. — Measured nozzle coefficient φ for nozzle No. 1, Fig. 21.

1. $p_1 = 10{\cdot}91$ at. abs.
2. $p_1 = 8{\cdot}90$ and $4{\cdot}92$ at. abs. } saturated steam.
3. $p_1 = 6{\cdot}92$ at. abs.

Fig. 33. — Measured nozzle coefficient for nozzles Nos. 1—4, Fig. 21.

1. With nozzle No. 1, 2. With nozzle No. 2,
3. With nozzle No. 3, 4. With nozzle No. 4.

Fig. 34. — Measured nozzle coefficient for nozzle No. 5, Fig. 21, for different initial temperatures.

1. $t_1 = 300$° C, 2. $t_1 = 250$° C, 3. t_1 = saturation.

nozzle, the efficiency is notably lower and the increase of φ to the right of the normal point greater than with the preceding nozzles. Consequently, the increase of efficiency by over-expansion is all the more pronounced when the friction in the nozzle is high; however, the maximum efficiency of an inefficient nozzle always remains below the efficiency of an efficient nozzle.

Fig. 34 gives some results obtained with nozzle No. 5. The efficiency remained high in this case, although with this nozzle a high pressure ratio was possible. With saturated steam the value of $\varphi = 0{\cdot}97$ was reached. This value increases with the superheat and reaches a maximum of $\varphi = 0{\cdot}976$ for an initial temperature of 300 ° C. Therefore, in a nozzle 150 mm long only about 5 % of the total heat is lost, i. e., only about half the losses assumed previously.[1]

Finally nozzles Nos. 6, 7 and 8 gave similar results, the maximum value of $\varphi = 0{\cdot}97$ being attained with saturated steam.

[1] Stodola, "Dampfturbinen," fourth edition, pp. 61—63.

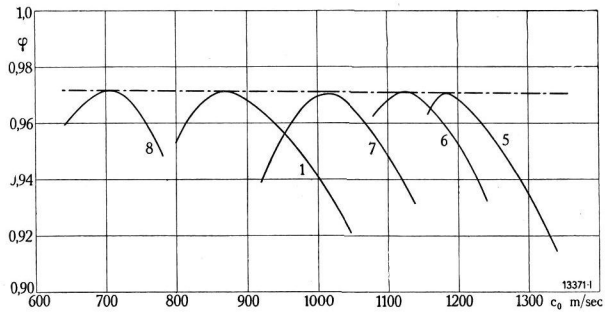

Fig. 35. — Comparison of the measured nozzle coefficients for nozzles having the same divergence ($tg\alpha_1 = 0{\cdot}1$), viz., Nozzles Nos. 1, 5, 6, 7, 8 (Fig. 21).

Fig. 35 allows of comparing the results for nozzles having the same divergence — the characteristics being drawn as functions of the rate of flow. Corresponding curves have the same characteristics, and the maxima of the latter are situated on an envelope which is also shown — in this case it is a slightly inclined straight line — and shows that when the rate of flow increases, the maximum efficiency slightly decreases.

Expanding nozzles of circular cross section are not used for turbines. The only technical application is for ejectors. Therefore, it does not seem of much use to investigate this kind of nozzle more fully here. The results obtained, however, will be of use for the determination of the friction on the nozzle walls at high rates of flow and of the supersaturation which appears on expansion of saturated steam.

II. DETERMINATION OF THE COEFFICIENT OF FRICTION AT HIGH RATES OF FLOW.

During expansion in a nozzle the flow is turbulent and not laminar. A survey of the various empirical results found for turbulent motion was given in these pages.[1] For the pressure drop in a cylindrical pipe the following formula was given:—

$$\Delta p = \lambda \frac{\ell}{d} \gamma \frac{w^2}{2g} \qquad (21)$$

λ in this case is not constant but depends on Reynold's coefficient $\frac{w\,d}{\nu}$. For smooth pipes Ombeck found that

$$\lambda = 0{\cdot}242 \sqrt[4{\cdot}47]{\frac{\nu}{w\,d}} \qquad (22)$$

Ombeck's experiments were undertaken, however, for velocities below that of sound. It is proposed to verify the exactitude of these formulæ for velocities greater than that of sound. The verification will first be undertaken with a conical (expanding) nozzle. The nozzle is divided into axial sections having a length of $\Delta\ell$ to which formula (21) is applied.

The force ΔR produced by friction on the nozzle walls is given by

$$\Delta R = f \cdot \Delta p = f \lambda \frac{\Delta \ell}{d} \gamma \frac{w^2}{2g}$$

The work of this force per second is evidently

$$\Delta W = f \lambda \frac{\Delta \ell}{d} \gamma \frac{w^3}{2g}$$

On account of the equation of continuity

$$G v = f w$$

and the identity

$$v \gamma = 1$$

it follows that

$$\Delta W = G \lambda \frac{\Delta \ell}{d} \frac{w^2}{2g}$$

The power per kg of steam is

$$\Delta W_1 = \lambda \frac{\Delta \ell}{d} \frac{w^2}{2g} \text{ kgm per sec.}$$

The expression can be simplified by writing

$$\beta = \frac{\lambda}{2g} \qquad (23)$$

and

$$\Delta W_1 = \beta \frac{w^2}{d} \Delta \ell \qquad (24)$$

Reynolds coefficient is given by

$$\frac{w\,d}{\nu} = \frac{10\,\gamma\,w\,d}{\mu_{abs}} \qquad (25)$$

Fig. 36 shows μ_{abs} as a function of the temperature; Fig. 37 gives β as a function of $\frac{w\,d}{\nu}$. From these curves the frictional work in a nozzle having an area of one sq. cm at the throat and a constant divergence of the conical portion ($tg\alpha_1 = 0{\cdot}1$) was calculated, the initial state of the steam being $p_1 = 12$ at. abs. and $t_1 = 300\,^0$ C. It was assumed that these formulæ were valid for velocities greater than that of sound, and the results obtained are plotted in Fig. 38. It will be noticed that, in the first part of the nozzle, the losses are very small, and that they increase towards the mouth. The curve A, Fig. 6[1], corresponds

[1] Revue BBC, No. 5, 1920 or BBC Mitteilungen, No. 12, 1919.

[1] See preceding footnote.

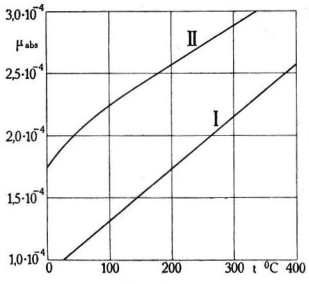

Fig. 36. — Absolute viscosity coefficient as a function of the temperature.

1. For steam, 2. For air.

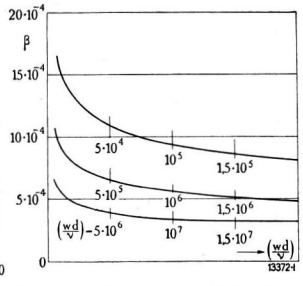

Fig. 37. — Coefficient of friction[1] $\beta = \frac{0{\cdot}0123}{\left(\frac{w\,d}{\nu}\right)^{0{\cdot}224}}$ as a function of Reynold's coefficient $\frac{w\,d}{\nu}$.

most closely to the conditions actually obtained. In any case for a small increase of velocity towards the mouth it is necessary to increase considerably the length of the nozzle — this is due to the fact that conical nozzles are used. If nozzles widening more rapidly towards the mouth were used, the friction losses would diminish, but, on account of the divergence of the jet, the radial components would augment — an increase of efficiency would therefore be problematical.

The calculations give values of φ varying from unity at the entrance of the nozzle to 0·97 towards the mouth. The nozzle considered in this case was assumed to be relatively long.

The value of $\varphi = 0{\cdot}97$ at the mouth was only obtained experimentally with nozzle No. 5, which was the longest nozzle tested, the divergence being $\operatorname{tg} \alpha_1 = 0{\cdot}1$. Shorter nozzles should, according to these calculations, have higher values of φ. It will be seen further on, that these discrepances are greatly due to supersaturation, which takes place in the nozzle. Nevertheless, it appeared advisable to verify more exactly for high velocities the law of friction given above.

For this purpose, nozzle No. 9 (Fig. 21) was designed. A special reamer allowed an insensible transition from a truncated cone to a cylinder to be made, so that the flow was not disturbed by sudden changes of direction. The expansion curve on an entropy diagram is given in Fig. 39. A B is the expansion curve for the conical portion, B C that for the cylindrical portion.

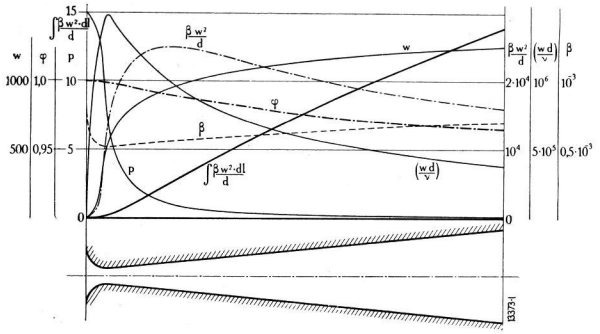

Fig. 38. — Variations of state as a function of the nozzle length.

B is determined since the efficiency of the conical part is known. C is determined by measuring the reactive force and the pressure at the nozzle mouth.

A slight increase of pressure takes place in the cylindrical portion. As the pressures p_2 and p_3 differ only slightly, it is possible to assume an average state along this section as given by D. The heat drop due to losses is given by Δi (Fig. 39). The average velocity in the cylindrical portion may be taken as being equal to the arithmetical mean of the entering and leaving velocities. The measurement of the losses allows β to be calculated by formula (24) and compared with the theoretical values, as obtained from Ombeck's formula

$$\beta_{th} = \frac{\lambda}{2\,g}\,\frac{0{\cdot}242}{2\,g}\sqrt[4{\cdot}47]{\frac{\nu}{w\,d}}$$

Nine tests were undertaken with this nozzle and the results are tabulated below.

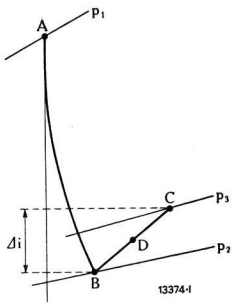

Fig. 39. — Variations of state in an entropy diagram.

TABLE III.

p_1 kg/cm²	t_1 degrees C	p_3 kg/cm²	p_2 kg/cm²	Δi Calories	wm m/sec	$\beta \cdot 10^3$	$\beta_{th} \cdot 10^3$	β/β_{th}
						β = coefficient of friction		
8·87	178·0	0·124	0·107	11·5	1106	8·56	7·0	1·22
8·89	250·0	0·113	0·103	10·5	1156	7·16	7·1	1·01
8·87	293·5	0·107	0·098	11·1	1192	7·12	7·21	0·99
10·84	202·0	0·146	0·131	10·5	1128	7·50	6·80	1·10
10·84	250·2	0·138	0·126	10·4	1161	7·02	6·90	1·02
10·84	292·5	0·131	0·120	11·2	1197	7·12	6·95	1·02
12·82	206·0	0·174	0·154	9·80	1134	6·95	6·50	1·07
12·82	249·5	0·164	0·149	9·55	1168	6·37	6·60	0·96
12·82	292·6	0·155	0·142	9·80	1204	6·16	6·61	0·93

From these the average value $\frac{\beta}{\beta_{th}} = 1{\cdot}035$ is obtained.

Although there are individual discrepancies up to 20 %, the average discrepancy is only 3·5 %. Therefore, these experiments seem to show that:

The laws of friction, established for velocities below that of sound, remain unaltered at higher velocities. In particular, the expression given by Ombeck for smooth walled cylinders is valid. The velocity of sound does not affect the laws of friction in pipelines, whereas the laws governing the air resistance to projectiles alter when the velocity exceeds that of sound.

Dr. de Freudenreich. (D. M.)

A NEW LINE OF TRANSFORMERS.

Decimal index 621. 314.

THE most important new features of this type of transformer are the *oil-conservator* and the *ratio-adjuster*. Full particulars as regards prices and electrical characteristics will be found in list T 5, August, 1921. A future article will deal fully with the favourable electric characteristics and the temperature rise of these transformers.

INTRODUCTION.

THE development of superpower stations, accompanied by extensions of the distribution systems, renders it more than ever imperative that all machines and apparatus used be reliable and efficient, with a low first cost and a short time of delivery. These considerations apply especially to transformers — which are employed in ever increasing numbers.

In order to be able to satisfy the foregoing requirements it is necessary, for manufacturing purposes, to classify transformers according to the service for which they are designed and to the mode of cooling.

The transformers hereafter described are of a design which has already proved itself satisfactory in all respects. On account of various new features they mark a decided advance in transformer construction. The new transformers are of the three-phase self-cooled oil-immersed type for outputs of 5 to 150 kVA, and for working tensions up to a maximum of 20 000 V. The robust design of these transformers, together with low overall dimensions, high efficiency and large overload capacity combined with low temperature rise, assures them a wide field of application. These transformers are suitable for use under all conditions, as they are arranged for erection on poles as well as indoors, and are further adapted for an oil-conservator being fitted if desired.

The ever extending adoption of the oil-conservator and the recognition of its advantages are greatly due to war conditions, under which highly refined transformer-oils were very hard to get or even unobtainable. The rapid decomposition of the oil was then effectively retarded by adding an oil-conservator to the transformer. The satisfactory behaviour of such apparatus has justified its retention and also its employment in future installations.

Former articles (see Revue BBC, 1917, No. 6, p. 131) have shown how important it is for safe working to use oils free from impurities. Hot oil in the presence of oxygen (air) oxidises, that is to say it becomes brown and the solid particles separate out, sludge is deposited on the windings and in the cooling passages, and the cooling process is hindered. It should be specially noted that the type of transformer under consideration has such a low temperature rise with normal working conditions and, moreover, is filled with an oil of such high quality, that the danger of oxidation need scarcely be considered. This danger is, however, to be feared when the transformer is frequently subjected to excessive overloads, which naturally overheat the oil. If, in consequence of large variations in the temperature of the surrounding air or the latter being damp, condensation inside the transformer occurs, an oil-conservator should certainly be employed.

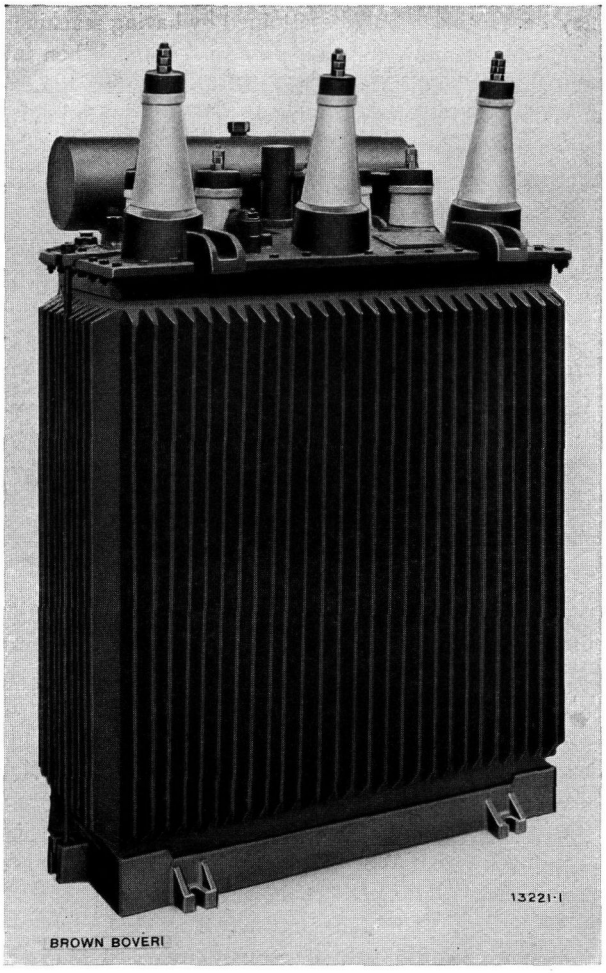

Fig. 1. — Three-phase oil-immersed transformer with oil-conservator, Type TK 50.

50 kVA, 20000/380 V, star/star zig-zag connections, 50 cycles.

THE OIL-CONSERVATOR.

When this is employed and the transformer is not unduly loaded, the oil will last almost indefinitely, and the conduction of heat away from the windings and core will therefore remain unimpaired.

With an oil-conservator (see Fig. 1) the transformer tank should be completely filled with oil. The oil-conservator is an expansion vessel, fitted at one side of the transformer cover, which takes up the extra volume of oil resulting from expansion when the temperature rises.

The position of the expansion vessel is important and must be such that the oil flows back into the transformer tank as soon as it cools, therefore the vessel must be situated above the transformer cover.

On this account the leads and the joints of the cover and also the pipe connections must be absolutely tight, whatever the temperature of the oil may be. This can only be attained by having machined joints and suitable tightly pressed packing. When the temperature rises the oil expands and enters the expansion vessel, where it cools rapidly. Consequently, only oil at a relatively low temperature comes into contact with air and oxidation is therefore obviated. The communication pipe is so shaped that the oil cannot circulate between the oil tank and the expansion vessel at steady load temperatures. Further, as this pipe projects some distance above the bottom of the vessel, the latter cannot be completely emptied; therefore moisture or impurities deposited on the bottom of the expansion vessel cannot find their way into the transformer. Water and other substances can be drawn off by a drain-cock. Whenever this is done, fresh oil, of a volume equal to that drawn off, must be added.

MECHANICAL DESIGN.

The transformer core consists of three upright core pieces of cruciform section (Fig. 2) connected together by yokes at the top and bottom. The joints are so made that the iron losses are reduced to a minimum, insulated bolts being used for fixing the parts together. The windings rest on substantial hardwood beams which serve to space and fix the transformer body in the oil tank; this is of special advantage when the transformer has to be transported. The windings are concentric, the high tension winding being situated outside. The first coils on the high tension side are specially well insulated so as to be able to withstand tension surges in the transmission system. The method of spacing the windings from the iron core and from one another

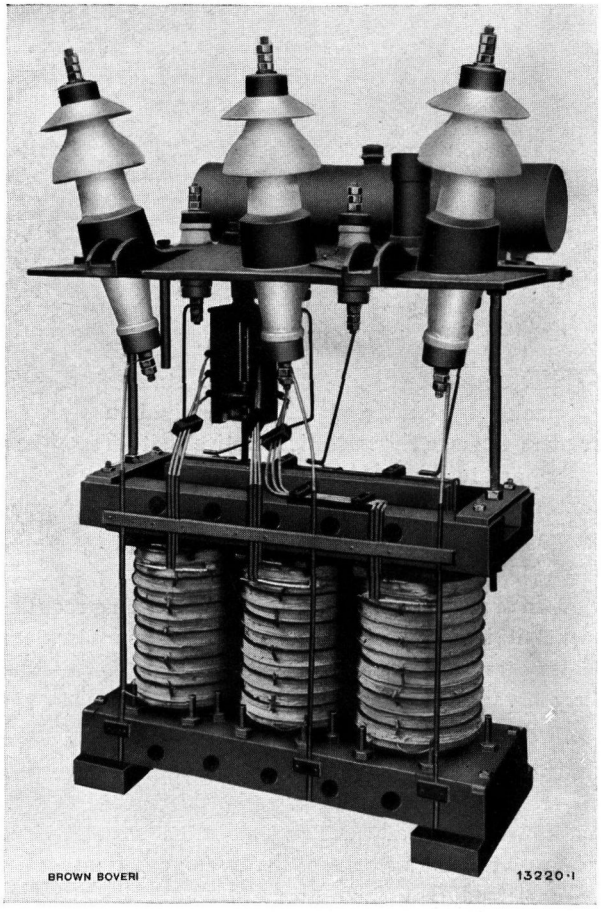

Fig. 2. — Three-phase oil-immersed transformer removed from its oil tank, Type TS 30 for erection on poles, and fitted with an oil-conservator.
30 kVA, 16000/380 V, 50 cycles.

has been given special attention. At the same time care has been taken that the surface of each coil remains as free as possible so that efficient cooling can take place. The cooling of the high tension coils is further assisted by specially shaped distance pieces between individual coils or pairs of coils. These increase the surface and form cooling ducts which notably assist in carrying off heat. The coils themselves are subjected after winding to a special treatment which renders them perfectly firm and rigid — a condition that remains permanent in spite of severe working conditions. The transformer proper is fixed to the cover by strong bolts and can be lifted with it, together with the leads, after loosening the bolts holding the cover to the tank. This arrangement is very convenient when connections have to be changed over inside the tank or repairs carried out.

The tank has sides of corrugated iron sheeting welded to a strong sheet-iron trough resting

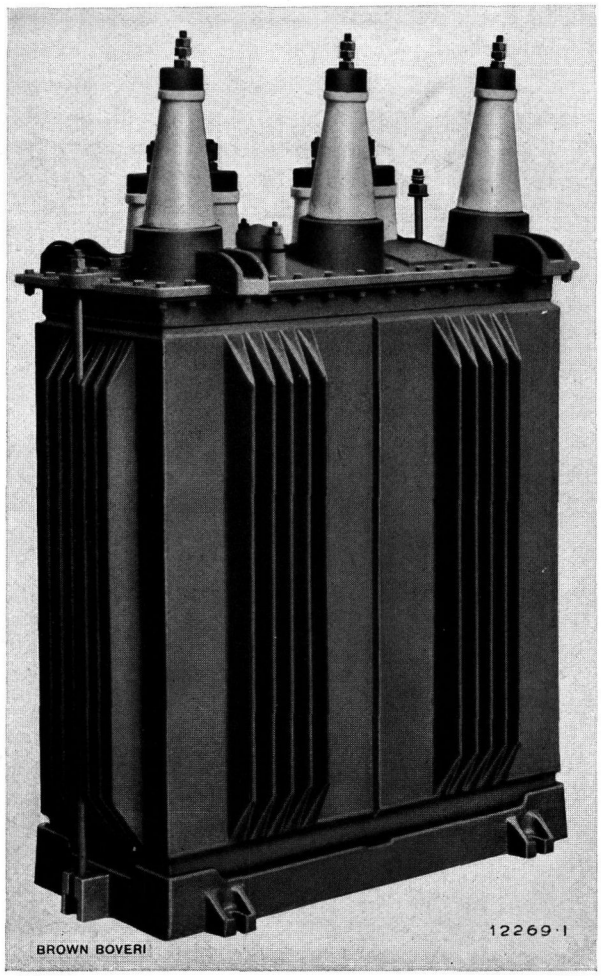

Fig. 3. — Three-phase oil-immersed transformer, Type T 20. 20 kVA, 10000/380 V, 50 cycles.

on a cast-iron baseplate. The tank is stiffened by angle irons. All joints and seams are autogenously welded; the tank, although of light weight, is therefore very strong and rigid. It is provided with a combined drain and test cock at the bottom, which allows either a large quantity of oil or only a small sample to be drawn off.

The cover is of cast iron, slightly dished, with facings to which the leads are fixed, as well as openings for the ratio-adjuster (to be described further on), oil-level indicator, ventilation and a tube for inserting a thermometer. When an oil-conservator is fitted, tapped holes are provided for the safety valve and the pipes leading to the expansion vessel. Snugs on the sides facilitate transportation. The under side of the substantial flange of the cover is machined, so that a tight joint is ensured. Transformers with an oil-conservator are further provided with special oil-resisting packings of a type which has proved entirely reliable. In transformers without an oil-conservator the space above the oil is connected with the outside air by a special arrangement which prevents, as far as possible, dust and damp from entering. The safety valve fitted to the cover of a transformer with an oil-conservator allows any oil gas which may be generated inside the tank to escape, without bringing the hot oil directly in contact with the outside air.

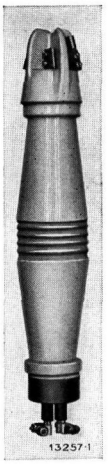

Fig. 4. — Tapping terminal for a 10000-volt oil-immersed transformer and a maximum current of 50 A.

The oil-conservator is a cylindrical expansion vessel (Figs. 1 and 2) with welded-on supports. Besides the pipe connections, it possesses an air outlet, a cock for drawing off samples of oil, and, on the top, an opening, which can be closed, for pouring in and controlling the oil. Suitable ventilation has been obtained here also by a specially constructed air inlet, which prevents, as much as possible, dust and damp from penetrating into the vessel.

The ratio-adjuster. Tapping terminals, as shown in Fig. 4 for instance, which permit changing-over from the outside, have been done away with in the new type; firstly, because it was not possible to construct a satisfactory terminal on account of the limitations of space and of the comparatively high tension, and secondly, as the various connections which are tapped off the first turns of the winding are those most exposed to tension surges. A ratio-adjuster placed inside the transformer tank, as now employed, renders the unscrewing and changing-over of connections superfluous, and only single-pole leads are necessary. It also makes it possible to take the tappings off parts of the winding less exposed to tension surges.

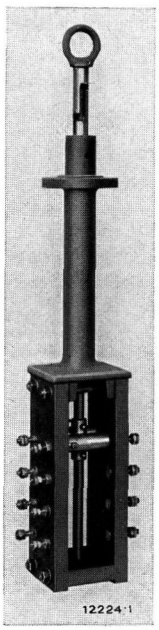

Fig. 5. — Ratio-adjuster for a three-phase oil-immersed transformer for maximum 10000 V and 50 A, star connected.

The ratio-adjuster (Fig. 5) consists of two vertical plates of insulating material carrying the contact pieces, the guide, the contact slide together with the switch rod and the operating handle with catch. Fig. 6 shows that with star/star connections, for instance, the points of equal pressure lie in the same horizontal plane. They are joined

to one another by the contact-slide, which is provided with contacts pressed on by springs. The adjuster is designed for a maximum current of 50 A, but has such liberally dimensioned and well-fitting contacts that the temperature rise and contact losses are negligible. Fig. 7 gives the results of tests on one of these adjusters. Although not in a position liable to tension surges it has ample spaces between contacts of the same phase and also between phases — the distances being calculated for the transformer test pressure.

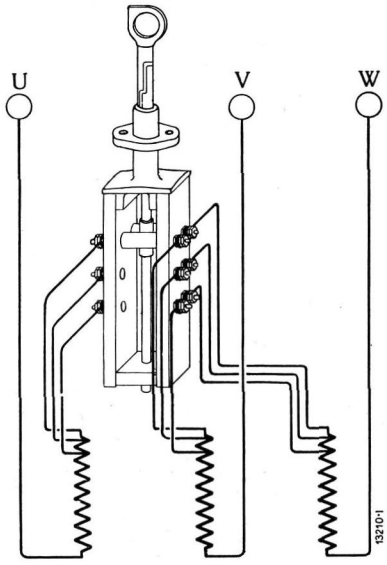

Fig. 6. — Diagram showing the ratio-adjuster, with two tappings per phase on the transformer and star connections.

Voltage regulation is obtained simply by moving the slide when the transformer is disconnected. The operation of the adjuster is as follows: —

(a) To increase the tension: The transformer is disconnected, the cap (Fig. 3) is removed by loosening the two nuts, the ring, which then becomes free, is drawn out as far as possible. By rotating this ring clockwise a little and pushing it back again the tapping for the next higher voltage is connected.

(b) To decrease the tension: The ring is drawn out as before and turned in the opposite direction, pulled out once more and turned further and then pushed home again.

Consequently, to every tapping step there corresponds a different position of the ring. The cap is so shaped that it can only be placed one way over the ring and occupies a different position for every step of the radio-adjuster when replaced. A pointer cast on to the cap indicates the position of the switch on a fixed scale, which can be read from the outside.

The foregoing shows that the operation and adjustment of the adjuster are extremely simple, and also that the safety and rapidity with which the pressure can be changed could scarcely be surpassed. Attention may also be drawn to the fact that the ratio-adjusters for transformers with oil-conservators are provided with a packing that prevents loss of oil when changing over.

E. Lapp. (D. M.)

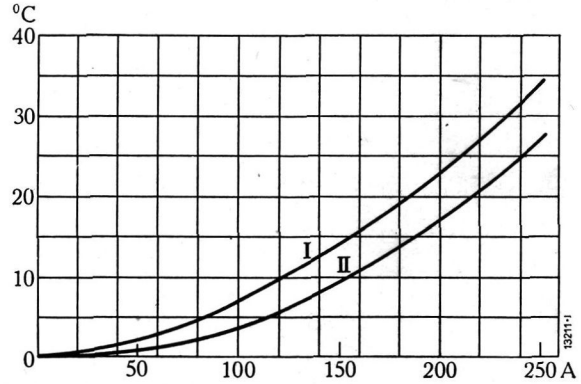

Fig. 7. — Curves showing the temperature rise at the contacts of the ratio-adjuster when immersed in oil.
Curve I: oil temperature 19° C.
Curve II: „ „ 70° C.

NOTES.

A mercury arc rectifier installation.

Decimal index 621.313.73.

THE Compagnie Industrielle pour l'Application des Procédés Brown Boveri, Brussels, has just obtained an important contract for the complete electrical equipment of a substation for Brussels, comprising mercury arc power rectifiers for supplying the D. C. power and lighting system.

In this article only a few general particulars are given, which will be supplemented, however, in a subsequent issue once the installation has been put into commission.

The substation is designed for the following technical data: —

H. T. three-phase current	5000 V.
Voltage variation	5 %.
Output on the D. C. side	800 kW.
Tension of the rectified current	230 V.

One of the conditions imposed by the specification was that, at a distributing point 200 m from the substation, the D. C. tension should remain constant (228 V) independently of the load. In order to meet this requirement the following factors had to be taken into account: —

The variations of the primary tension.

The voltage drop in the installation.

The ohmic drop in the underground cables between the rectifiers and the distributing point 200 m away.

A three-phase oil-immersed induction regulator, connected to the primary circuit of the transformers, was installed. This apparatus regulates the A. C. voltage within the limits required to obtain a constant tension of 228 V at the D. C. distributing point. The control is carried out electrically by means of a Brown Boveri quick-acting pressure regulator in such a way as to obtain an over-compound load characteristic.

The 5000-volt H. T. current is led by two three-phase cables, of 30 sq. mm section, to the induction regulator through the usual high-tension apparatus. It is then distributed by bus-bars to two six-phase oil-immersed transformers which reduce the tension to the value required on the A. C. side of the rectifiers.

These transformers are built specially for feeding rectifiers; they have large leakage and also high short-circuit reactance. The no-load losses are low so that, apart from other factors, the overall efficiency remains high even at light loads.

There are four six-phase rectifiers for 900 A each, connected in parallel on the D. C. side. Equal distribution of the load is attained by the use of anode reactance coils with compensating windings, which are placed between the secondary winding of the transformer and the rectifier anodes.

The neutral point of the transformers, to which cathode reactance coils are connected, constitutes the negative pole of the installation. The positive pole is formed by the cathodes of the rectifiers.

The D. C. distribution system comprises five three-wire distribution mains all for the same power.

For the three-wire arrangement a balancer set is employed consisting of two shunt wound machines coupled together and connected across the rectifier bus-bars. The out-of-balance current can attain about 10 % (360 A) in the neutral wire. The balancer set has therefore been designed for about 25 kW.

The complete installation is guaranteed to carry safely the following overloads: —

25 % for half an hour, 40 % for 3 minutes, 70 % for short periods.

Attention may be drawn to the fact that mercury arc power rectifiers have many advantages over rotary converting plant, such as very high efficiency, simplicity of operation and low upkeep.

Further, on account of the absence of mechanical inertia and commutators, they are the type of plant which is the least sensitive to sudden peaks, whilst commutation troubles as always met with on overloads are done away with.

Bossy. (D. M.)

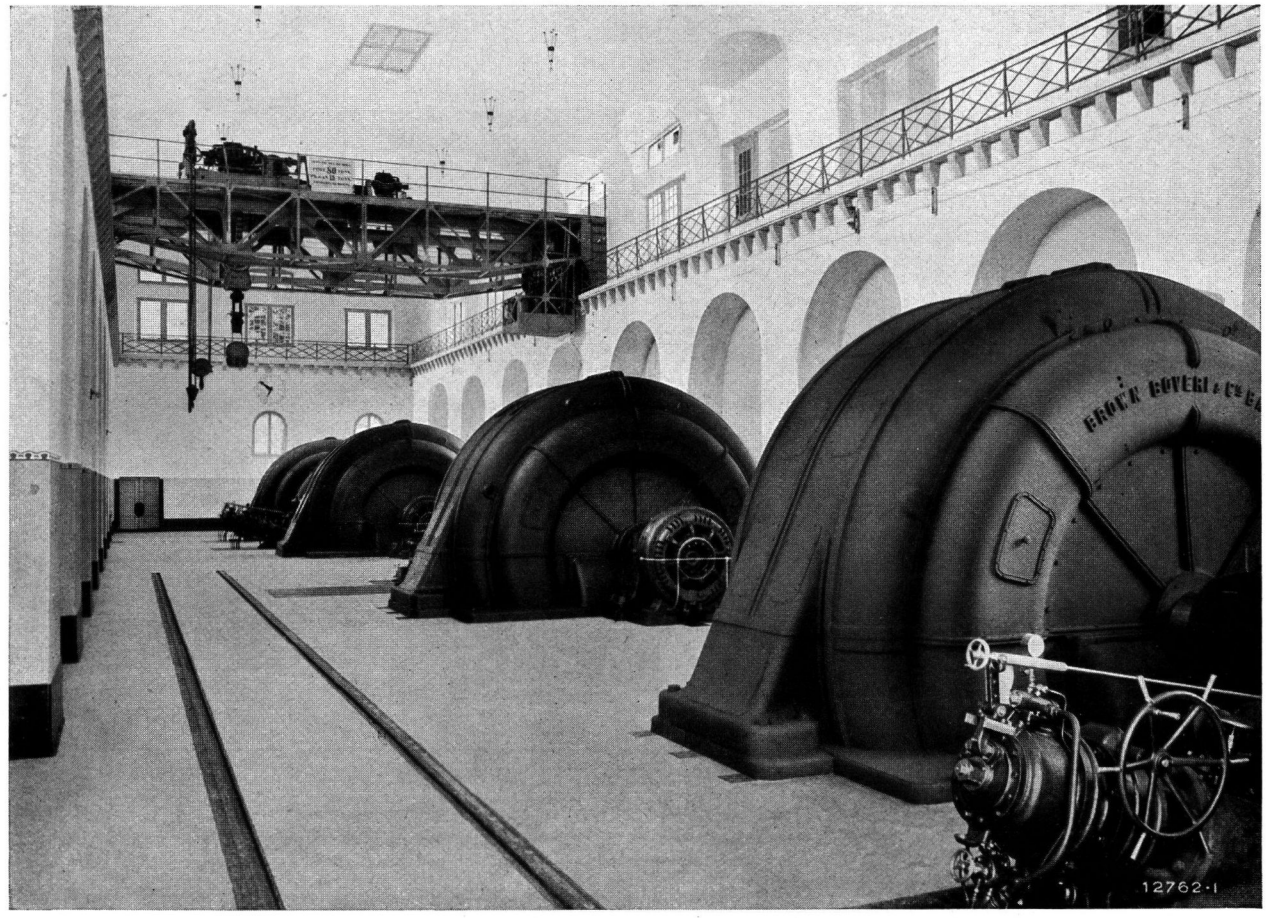

Swiss Federal Railways. Machine room of Ritom power station.

Issued by BROWN, BOVERI & CO., BADEN (Switzerland). Printed by Kreis & Co., Basle.

BROWN, BOVERI & CO.

BADEN (SWITZERLAND)

WORKS: BADEN AND MUNCHENSTEIN (SWITZERLAND)

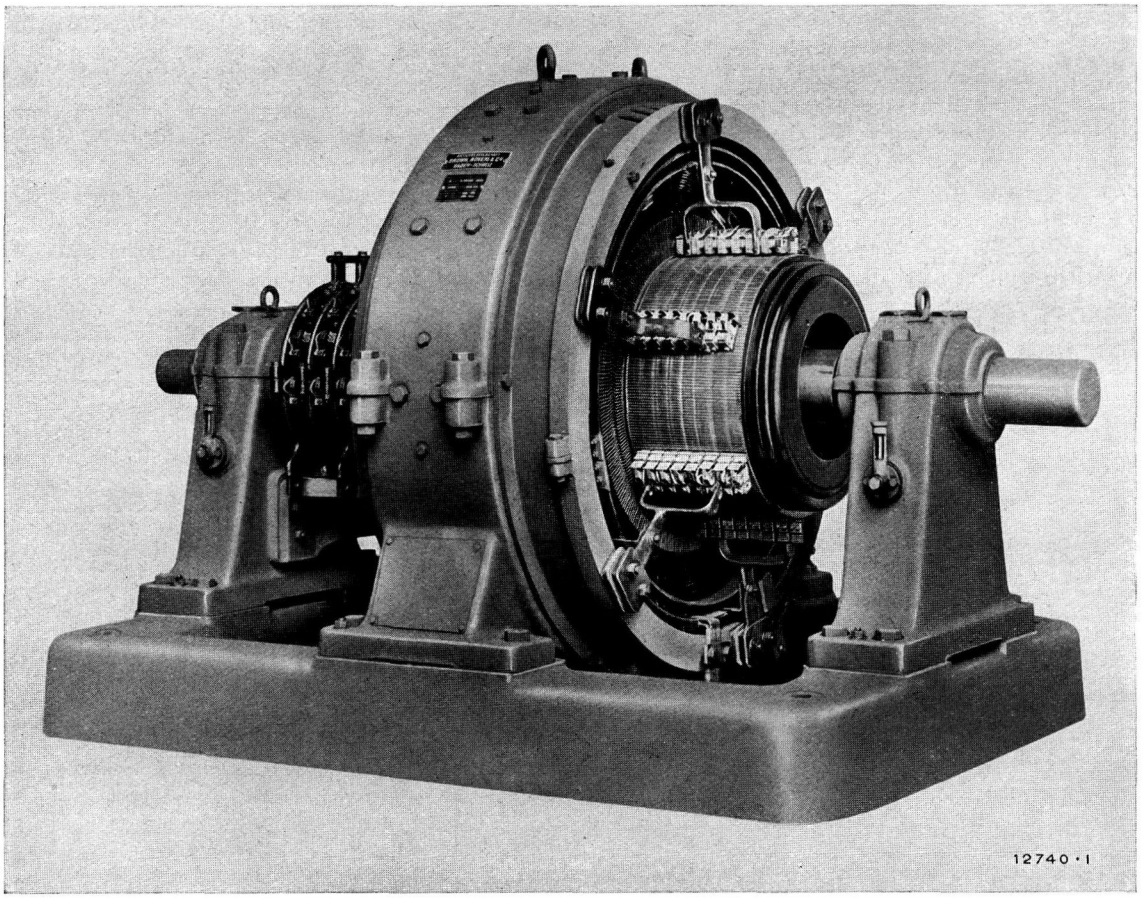

SIX-PHASE ROTARY CONVERTER, 750 kW, 550–600 V, 1000 r. p. m.

ROTARY CONVERTERS
MOTOR - GENERATORS
POWER RECTIFIERS